Exp Brain Res (2000) 131:477–490
Digital Object Identifier (DOI) 10.1007/s002219900317

RESEARCH ARTICLE

Colum D. MacKinnon · Mary C. Verrier
William G. Tatton

Motor cortical potentials precede long-latency EMG activity evoked by imposed displacements of the human wrist

Received: 16 August 1999 / Accepted: 07 December 1999 / Published online: 24 February 2000

Abstract Rapid angular displacements of the wrist evoke cerebral potentials that precede the onset of the long-latency electromyographic (EMG) activity generated in muscles stretched by the displacement. The initial segment of the long-latency EMG activity (termed the M2 response) is thought to be mediated by a transcortical reflex. We used dipole source analysis to examine the source generators of the early components of the cerebral potentials and their relationship to the timing and magnitude of the M2 response. Subjects (n=10) were presented with instructions to either actively flex or extend the wrist in response to a torque motor-imposed extensor displacement or allow the wrist to be passively extended. Electroencephalographic (EEG) recordings were obtained from 32 scalp-surface electrodes, and EMG was recorded from the wrist flexors and extensors. For all three tasks, the M2 response was preceded by cerebral potentials that could be explained by a three-dipole model. One source generator localised to deep within the cerebrum, and the other two localised to the region of the contralateral sensorimotor cortex. We used the P20-N20 dipole evoked by electrical stimulation of the median nerve at the wrist, corresponding to synaptic activity within cortical area 3b, as a local spatial reference to examine the contributions of the pre- and postcentral cortex. This analysis showed that one of the sensorimotor dipoles was consistently located anterior to the P20-N20 dipole at a displacement (average 11.5 mm) appropriate for a generator originating within the deep layers of area 4 on the anterior bank of the central sulcus. The orientation of this dipole was also consistent with a precentral generator and not a reversal of the potentials generated by input to area 3b. The time course of the area-4 dipole moment (onset =35 ms, peak =54 ms) was appropriate to reflect synaptic activity onto corticospinal neurons whose descending volleys mediate the M2 response. Comparisons across tasks showed that the magnitude of the M2 was modulated with task instruction, being largest with active and smallest with passive resistance. In contrast, the magnitude of the early evoked potentials (up to 75 ms) did not grade across tasks. We interpret these results as suggesting that instruction-dependent modulation of the M2 response occurs downstream from inputs to the primary motor cortex.

Key words Evoked potentials · Primary motor cortex · Long-latency stretch reflex · Dipole source analysis

Supplementary material for this paper can be obtained electronically by using the Springer LINK server located at http://dx.doi.org/10.1007/s002219900317

C.D. MacKinnon · M.C. Verrier · W.G. Tatton
Department of Physical Therapy, University of Toronto, Toronto, Canada

C.D. MacKinnon · M.C. Verrier · W.G. Tatton
Department of Physiology, University of Toronto, Toronto, Canada

M.C. Verrier
Department of Rehabilitation Science, University of Toronto, Toronto, Canada

C.D. MacKinnon · W.G. Tatton
The Clarke Institute of Psychiatry, 250 College St., Toronto, Canada

C.D. MacKinnon (✉) · W.G. Tatton
Department of Neurology, Mount Sinai School of Medicine, One Gustave L. Levy Place, New York, NY 10029–6574, USA
e-mail: colum_mackinnon@smtplink.mssm.edu
Tel.: +1-212-2417310, Fax: +1-212-3481310

Introduction

Rapidly imposed joint angular displacements elicit both short- and long-latency electromyographic (EMG) activity from the stretched muscle groups (Hammond 1954). The timing of the short-latency EMG activity, termed the M1 response (Tatton and Lee 1975), is appropriate to be largely mediated by monosynaptic input from group-Ia afferents. The long-latency response begins before volitional EMG activity and, therefore, is thought to also be reflex in origin.

The balance of evidence suggests that the initial component of the long-latency response (M2 response)

evoked in the distal musculature of the upper limb is predominantly mediated by a transcortical pathway through the contralateral primary motor cortex (Lee and Tatton 1975; Tatton et al. 1975; Marsden et al. 1977; Wiesendanger and Miles 1982; Cheney and Fetz 1984; Verrier et al. 1984; Day et al. 1991; Matthews 1991; Palmer and Ashby 1992). In contrast, long-latency responses evoked in proximal muscles receive little, if any, contribution from the primary motor cortex (Lenz et al. 1983a, 1983b; Tatton et al. 1983; Thilmann et al. 1991; Fellows et al. 1996) and are thought to be generated by inputs from slow-conducting or polysynaptic segmental pathways (Matthews 1991). Lee and Tatton (1982) have further shown that the M2 evoked in the wrist flexors may be dependent upon convergent input from two or more separate pathways, implying that proximal and distal muscles receive differentially weighted contributions from segmental and supraspinal pathways. Thus, the relative contribution of transcortical pathways to the generation of the M2 in humans remains unclear.

In addition to the segmented EMG response, rapidly imposed joint displacements also evoke cerebral potentials, which can be recorded from the scalp surface (Papakostopoulos et al. 1974; Conrad et al. 1984; Abbruzzese et al. 1985; Crammond et al. 1985; Ackermann et al. 1986; Goodin et al. 1990; Desmedt and Ozaki 1991; Tarkka and Hallett 1991; Goodin and Aminoff 1992; Mima et al. 1996, 1997). The onset of these potentials precedes the onset of the M2 and, therefore, the early components of these potentials might reflect synaptic activity onto neurones that mediate a transcortical reflex. Studies that have examined the relationship between these potentials and the M2 have been confined to measurements of the timing and magnitude of scalp-surface potentials from a limited array of electrodes without regard for the underlying source generators (Abbruzzese et al. 1985; Ackermann et al. 1986; Conrad et al. 1984; Goodin et al. 1990; Goodin and Aminoff 1992). Studies examining the source generators of the potentials evoked by displacements of the distal upper limb have reported inconsistent findings. Generators have been attributed to synaptic activity principally confined to the areas 1, 2 and 3a of the contralateral, primary somatosensory cortex (Mima et al. 1996; Bötzel et al. 1997), while others have proposed that activity within the pre- and postcentral gyri contribute to the scalp-surface potential (Desmedt and Osaki 1991). Similarly, recordings from subdural electrodes in a patient with epilepsy (Mima et al. 1997) were unable to differentiate potentials arising from the pre- or postcentral cortex. Therefore, the source generators of the cerebral potentials evoked by imposed joint displacements, and their relationship to the long-latency EMG activity, remain unclear.

Discrepancies in the interpretation of the underlying source generators may result from the close juxtaposition of the posterior and anterior banks of the central sulcus and temporal overlap of synaptic activity evoked in the two regions. Differentiation of source generators within adjacent gyri requires the use of intracranial near-field and laminar recordings. These techniques have been used to show that the P20-N20 potential evoked by electrical stimulation of the median nerve at the wrist is generated by synaptic input to neurones within area 3b of the postcentral cortex (Allison et al. 1991). Furthermore, it has been shown that the source generator of the P20-N20 potential can be reliably localised in humans using dipole source analysis (Buchner et al. 1995; Kristeva-Feige et al. 1997; Grimm et al. 1998). Accordingly, we used the location of the P20-N20 dipole as a local spatial reference for the localisation of the distal upper-limb representation within area 3b of the postcentral gyrus.

The purpose of the following experiments was to examine the location, magnitude and timing of the source generators of the cerebral potentials evoked by imposed displacements of the human wrist and their relationship to the M2 response. The timing and amplitude of the evoked potentials were compared across tasks that differed in the magnitude of the M2 response, but not in the magnitude of the M1 or imposed velocity (Lee and Tatton 1975). Our findings showed that the cerebral potentials evoked by imposed wrist displacements were generated, at least in part, by synaptic activity within area 4 on the anterior bank of the central sulcus. Furthermore, the timing of the cerebral potentials was appropriate for area 4 neurones to contribute to the mediation of the M2 response. However, the absence of task-dependent modulation of the cerebral potentials, despite the presence of marked changes in the magnitude of the M2 across tasks, suggests that modulation of the M2 occurs downstream from inputs to the primary motor cortex.

Materials and methods

Subjects

Ten subjects (six males, four females, age range 22–37 years) were recruited for the study after obtaining informed consent. Experiments were approved by the Review Committee on the Use of Human Subjects at the University of Toronto. All subjects were right hand dominant and had no history of upper-arm injury or neurological disorders.

Electroencephalograph and electromyograph recordings

Electroencephalographic (EEG) scalp recordings were obtained from a montage of 32 gold-disk electrodes placed on the surface of the scalp at standard international 10–20 electrode sites including: the nasion, FP1, FP2, F7, F3, Fz, F4, F8, FC5, FC1, FC2, A1, T3, C3, Cz, C4, T4, CP5, CP1, CP2, T5, P3, Pz, P4, T6, O1 and O2 (see Figs. 2 and 4). Additional electrodes were placed over the lower canthi of the right and left eyes, the inion (CBz) and bilaterally at the midpoint between the mastoid process and CBz (CB1 and CB2). Scalp/electrode impedance was kept below 7 kΩ. All EEG signals were differentially amplified (bandwidth 0.1–2000 Hz, 3 dB/oct; gain =20 K ±1%, common mode rejection ratio ~100 dB) with respect to a reference electrode over the right mastoid process. Bipolar surface EMG recordings were obtained from electrodes placed 2 cm apart (centre-to-centre) over the motor points of flexor carpi radialis (FCR) and extensor digitorum communis (EDC) of the right arm and differentially amplified (gain =1–10 K;

CMRR ~100 dB; bandpass =20–1000 Hz). All signals were sampled at 1000 Hz using a 12-bit analog-to-digital converter and data-acquisition software (Neuro Scan).

Following data acquisition, EMG data were baseline corrected using the 100 ms time period preceding torque onset, full-wave rectified and averaged across epochs. Onset of the M1 segment of the EMG response was defined as the time point when the rectified EMG exceeded three standard deviations from the mean rectified baseline activity calculated from 60 to 40 ms prior to torque onset. Onset of the M2 was defined as the time point when the falling phase of the M1 segment reached a minimum and was followed by a period of increased activity for greater than 10 ms. The magnitudes of the M1 and M2 EMG segments were quantified by integrating the EMG (IEMG) over a 20 ms time period from the onset of the segment and normalising these values to the IEMG over a 20 ms time period (–60 to –40 ms) preceding torque onset. Similarly, the IEMG over periods of voluntary muscle activation were quantified over the time interval from 140 to 160 ms after the onset of the step-load. Differences in the timing or magnitude of the peak joint displacements, velocity and EMG or EEG variables were examined across tasks using the Mann-Whitney Rank Sum Test (Siegel 1956) and were considered significant at the $P<0.05$ level.

Task

Subjects sat comfortably in a chair and grasped a handle that was coupled to the shaft of a torque motor. The subject's right shoulder and elbow were in approximately 45° of abduction and 75° of flexion, respectively. The flexion-extension axis of the wrist joint was aligned to the centre of rotation of the shaft of the torque motor. The position of the lower arm was restrained in a cuff and the hand was held fixed in a natural semi-supinated position while grasping the handle.

Rapid angular displacements of the wrist from a central hold position were delivered using a DC brushless torque motor (Aeroflex Laboratories DC Brushless Torque Motor, Model T2 W) that produced a 1.0±0.1 Nm moment of 1 s duration in the direction of wrist extension. The delay between the onset of the computer-controlled trigger pulse (beginning of data collection) and onset of angular movement of the torque shaft was 3–4 ms. A potentiometer, fixed to the torque motor shaft, measured angular displacement and a strain gauge, mounted along the shaft of the handle, measured the torque on the handle in response to the step-loads.

An array of computer-controlled light-emitting diodes (LEDs) was placed 60 cm in front of the subject in the midline of their field of view. Subjects were instructed to maintain their wrist in a neutral position within an angular target zone to ±5° between trials. A light was illuminated when the wrist joint angle was outside this target zone. A random delay period of 2.0–4.5 s was introduced between perturbations to allow subjects time to move their wrist within the target zone. Once within the target zone, subjects were presented with one of three task instructions, coded by the colour of an LED array (instruction lights), for 750 ms. The three task instructions were either: (1) resist the wrist extension displacement by flexing the wrist (RESIST task), (2) extend the wrist in the same direction as the wrist extension displacement (EXTEND task), or (3) do not resist the wrist extension displacement (PASSIVE task). For the RESIST task, subjects were instructed to respond as rapidly as possible to the imposed displacement by resisting the extensor torque and by moving the handle back to within the central target zone. The EXTEND task required subjects to extend their wrist as rapidly as possible to the end of the range of motion and to hold that position until the torque step-load stopped. For the PASSIVE task, subjects were instructed to allow the torque motor to passively move the wrist into the extended position without exerting active resistance. A random delay period of 1.5–4.5 s was introduced between the end of the visual instruction and onset of the torque step-load to minimise early voluntary responses in anticipation of the wrist perturbation.

Care was taken to ensure that feedback of wrist position and torque step-load onset was provided by proprioception alone. Visual feedback of wrist position was eliminated by shielding the subject's arm and the torque motor apparatus from view. A square-wave pulse was sent in parallel with the trigger pulse that grounded the centre target light for a 300-ms duration to ensure that the target-zone light did not cue movement initiation. Auditory cues were eliminated by the use of white noise transmitted through earplugs inserted into both ears.

Epochs were collected from 100 ms prior to perturbation onset to 412 ms after the onset. Trials with eye movement artefacts occurring within the first 100 ms after the onset of the torque impulse were rejected before averaging. A minimum of 200 artefact-free epochs was collected for each task condition. After data acquisition, all trials accepted for each condition were baseline corrected (–100 to –1 ms), averaged and low-pass filtered (dual-pass, 250 Hz, 24 dB/oct).

Artefacts produced by the electromagnetic fields evoked by the torque motor were reduced by housing the motor within a shielded box of 1/8" iron. The artefact was stable and reproducible and consisted of a uni- or bimodal waveform with a maximal amplitude of 3.2 μV (at FC5) and a duration of up to 39 ms. For this reason, an additional set of 200 control trials was obtained with the subject relaxed and unattached to the torque motor apparatus. These trials were averaged and subtracted from the average responses for each task condition.

Dipole source analysis

The source generators of the cerebral evoked potentials were modelled using spatio-temporal dipole source analysis (Brain Electric Source Analysis version 2.0; for a review, see Scherg 1990). The effects of volume conduction of the field potentials to the surface of the scalp were modelled using a three-shell spherical head model (head radius 85 mm; scalp thickness 6 mm, conductivity 0.33 mho/m; bone thickness 7 mm, conductivity 0.0042 mho/m; CSF thickness 1 mm, conductivity 1 mho/m; brain conductivity 0.33 mho/m). Equivalent current dipoles were quantified based on their location within the spherical head model, orientation with respect to a vertical and transverse axis and a magnitude reflecting the equivalent dipole moment. The origin of the Cartesian coordinate system within the spherical head model corresponds to the centre of the head with an x-axis (medial/lateral) pointing to the right through T4, a y-axis (anterior/posterior) through FPz and a z-axis (dorsal/ventral) upward through Cz. Orientation of the dipole vector is reported as theta (θ) and phi (ϕ), corresponding to polar angles with respect to the vertical (z) and medial/lateral (x) axis, respectively (for further details, see MacKinnon et al. 1996).

Prior to dipole source analysis, the averaged epochs were average referenced and digitally filtered (low-pass 250 Hz, 24 dB/octave, dual-pass filter). All timing and magnitude data were determined from the dipole moments generated from the unfiltered data to ensure that distortions produced by digital filter phase shifts were avoided. Dipole solutions were generated by iteratively changing both the location and orientation of dipoles within the head model to yield a least- squares best fit to the EEG surface signals over the specified time range. Stable dipole solutions were internally validated based on three primary criteria: (1) the residual variance (RV, expressed as a percentage over the fitting interval) between the dipole model and the scalp surface EEG, (2) by testing for the contributions from other regions within the cerebrum using an orthogonal regional source, (3) and by assessing the anatomical and physiological feasibility of the solution.

Somatosensory-evoked potentials to electrical stimulation of the median nerve

Somatosensory-evoked potentials (SEPs) were elicited by electrically stimulating the median nerve using surface electrodes placed over the nerve at the wrist crease, with the cathode placed proximal

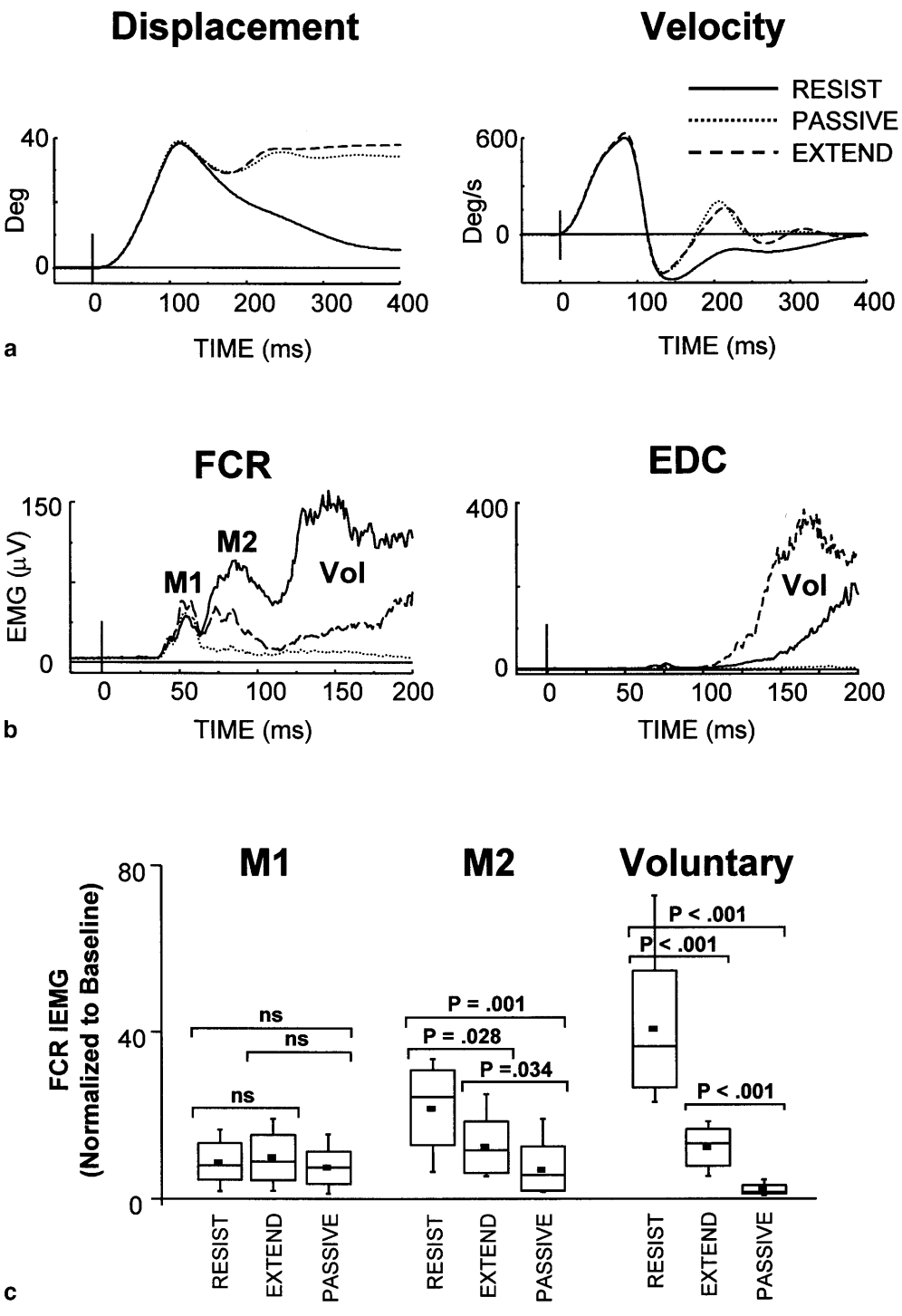

Fig. 1 **a** The group, mean angular displacements and velocities produced by wrist-extension step-loads across all three tasks (*RESIST unbroken line*, *EXTEND dashed line*, and *PASSIVE dotted line*, see Materials and methods for task descriptions). Note that the angular displacements and velocities generated over the first 75 ms after the onset of the step-load were the same across tasks. Positive values are extensor. **b** Electromyograph (*EMG*) responses in flexor carpi radialis (*FCR*) and extensor digitorum communis (*EDC*) over the first 200 ms following torque onset in a single subject. The average rectified EMG responses for the three tasks have been overlaid. The plot on the *left* demonstrates the segmentation of the FCR response into a short-latency (*M1*), long-latency (*M2*) and later voluntary (*Vol*) response. **c** Summary of the magnitude of the integrated EMG (*IEMG*) responses in FCR across all subjects and tasks. The *box plots* show the mean (■), median (*unbroken line*), 3 SE (□) and 99th percentile values (⊥). Note that the M2 and voluntary responses were significantly different across tasks, whereas the M1 responses were of the same magnitude across tasks

to the anode by a distance of 2 cm centre-to-centre. Square-wave pulses of 0.2 ms duration were delivered at random time intervals between 1 and 2 s and at an intensity sufficient to elicit activation of the thenar musculature and a small twitch of the thumb. Epochs were recorded from 50 ms prior to 150 ms after the stimulus. Trials with excessive artefacts due to eye movements or head muscle contractions were rejected before averaging. A total of 300–400 epochs were collected, averaged, baseline corrected (–50 to –1 ms) and filtered (high-pass: 5 Hz, 6 dB/oct, forward filter; low-pass: 250 Hz, 24 dB/oct) prior to dipole source analysis. The dipole fitting strategy adopted to model the source generators of the early components of the SEP is described in the results section below.

Results

Kinematics of rapid angular displacements of the wrist

The step-loads induced by the torque motor generated a rapid angular displacement of the wrist from the neutral hold position to an average peak wrist extension angle of approximately 40° in 114 ms (Fig. 1a). The average peak angular velocities across subjects were 604±67 (mean ±1 standard deviation), 606±73 and 631±32°/s for the

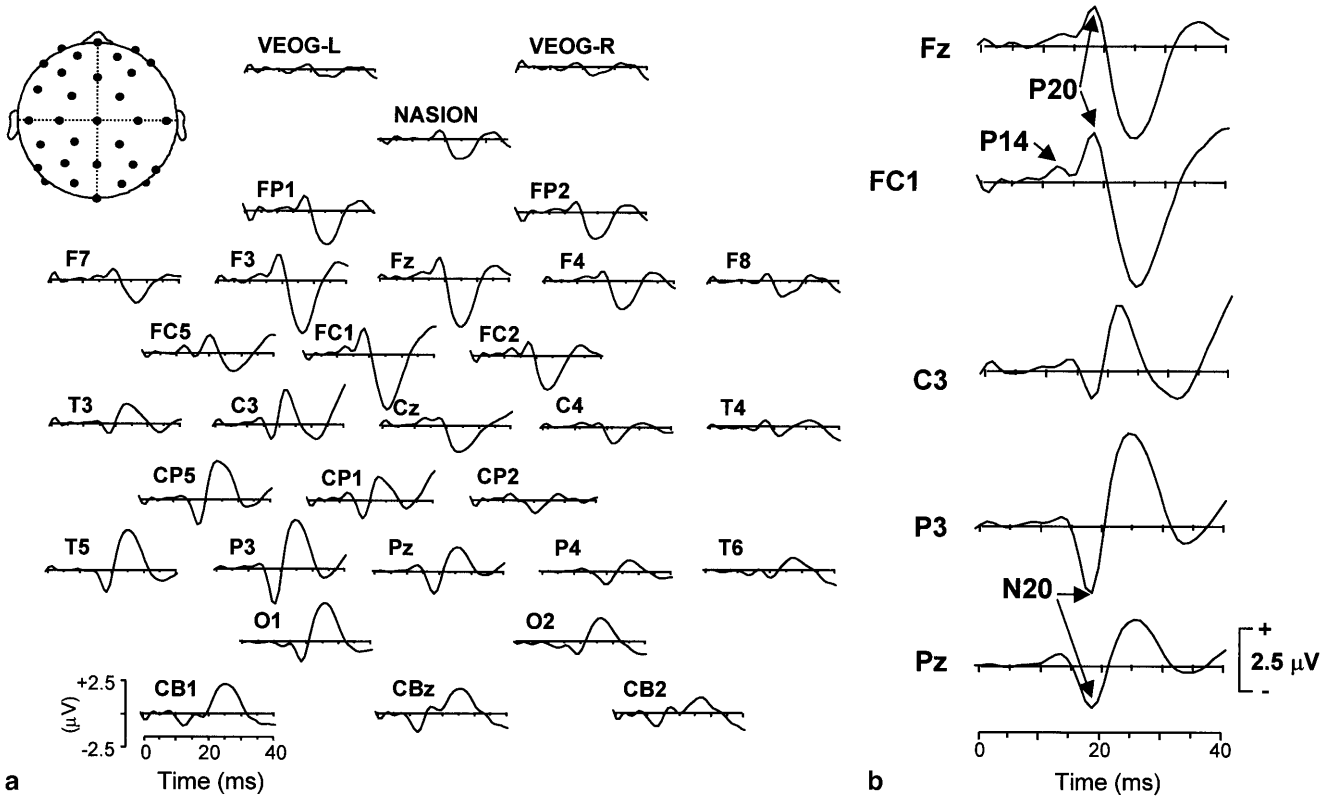

Fig. 2a, b Scalp-surface topography of the SEPs resentative subject. The cerebral potentials at 31 electrodes encompassing the surface of the scalp are shown relative to an average reference derived from all electrodes. A schematic cartoon of the placement of the electrodes on the surface of the head is shown at the *top left*. Note the early frontal positivity at FC1, Fz and F3 and parietal negativity at CP5, CP1 and P3, corresponding to the P20-N20 potential. Onset of stimulation was at time = 0 ms

RESIST, EXTEND and PASSIVE tasks, respectively. There were no significant differences across tasks (P>0.05) in the angular displacements or velocities imposed by the step-loads over the first 75 ms after the onset of the step-load.

EMG responses to rapid angular displacements of the wrist

Rapid angular extensor displacements of the right wrist generated distinct M1 and M2 responses in FCR in all subjects. An example of the average rectified EMG response evoked across tasks for both FCR and EDC is shown for a single subject in Fig. 1b. A clear separation between the activity labelled M1 and M2 and also between M2 and the onset of the voluntary activity was observed in this subject. In other subjects, the separation between M2 and voluntary activity was less pronounced and, in some cases, was only represented by a small inflection. The mean onset latencies across subjects for the M1 segment were 32±2, 32±2 and 32±3 ms for the RESIST, EXTEND and PASSIVE tasks, respectively. The corresponding onset latencies for the M2 segment were 60±5, 60±6 and 62±6 ms. The onset of EDC EMG activity for the EXTEND task occurred an average of 87.7±9.5 ms after torque onset. Assuming that the onset of EDC activity for the EXTEND task reflects the earliest onset of voluntary activity, the timing of the FCR M2 response was consistent with the initial portion of the long-latency EMG activity being generated by a reflex response.

The M2 response graded across tasks, being largest for the RESIST task and smallest for the PASSIVE task (Fig. 1c). The M2 segment was significantly increased for the RESIST task relative to the responses observed for both the EXTEND (P=0.028) and PASSIVE (P=0.001) tasks. Similarly, the M2 responses for the EXTEND task were significantly increased relative to the PASSIVE task (P=0.034). In contrast, the magnitude of the M1 responses were not significantly different across tasks (P>0.60). The magnitude of the voluntary responses to the imposed displacement also graded significantly (P<0.001) across tasks, with the largest IEMG occurring in FCR for the RESIST task, a moderate amount of activity for the EXTEND task and comparatively little activation for the PASSIVE task. No significant differences were observed in baseline FCR EMG activity preceding the onset of the step load across tasks (P>0.27); therefore, differences across tasks could not be accounted for by differences in pre-existing baseline EMG activity.

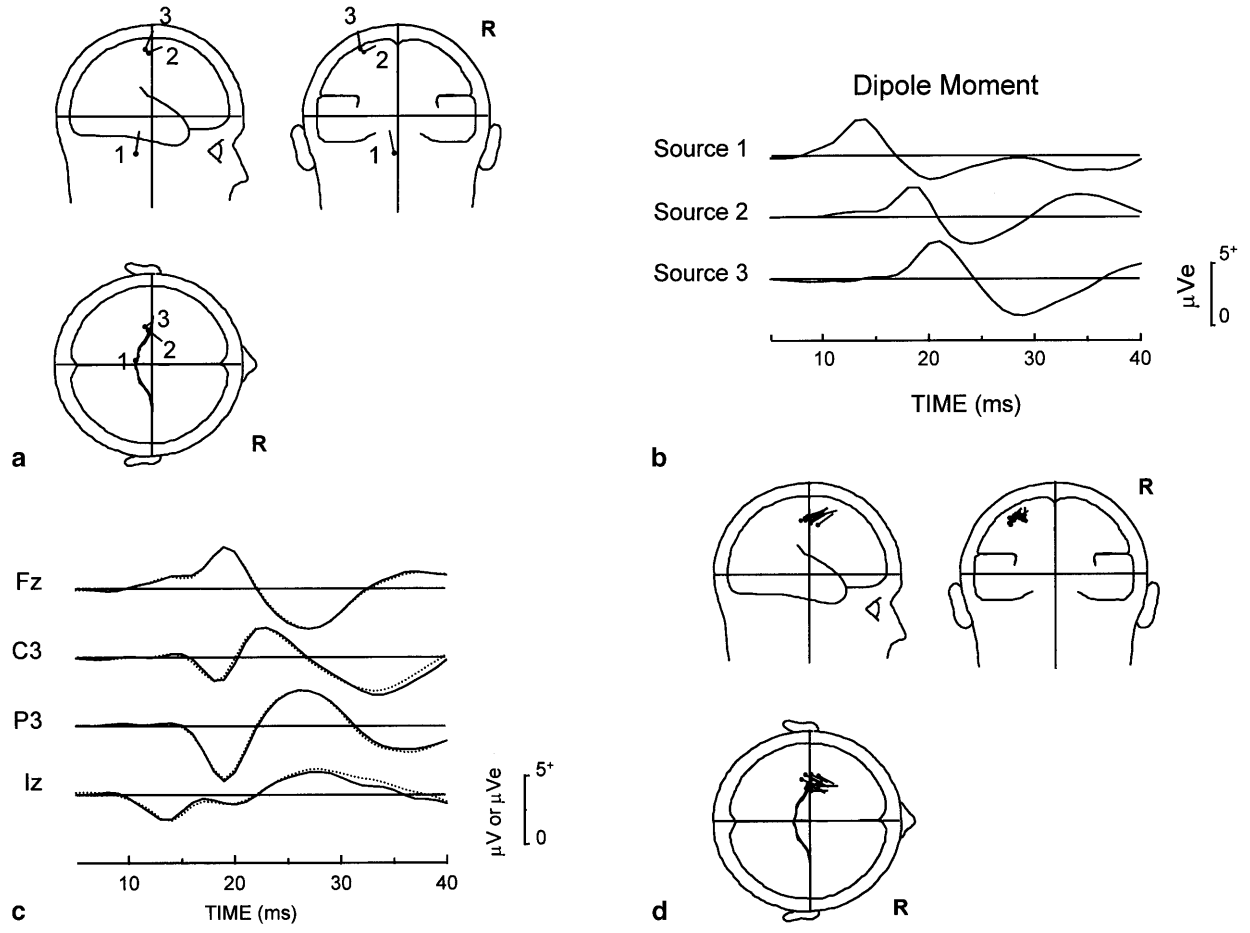

Fig. 3a–d Example of the dipole fitting strategy used to model the source generators of the early components of the median-nerve somatosensory-evoked potentials (SEP_{MNs}) in a representative subject. **a** The head models on the *upper left* show three orthogonal views of the location and orientation of the three dipoles (*1*–*3*) that modeled the scalp-surface potentials. **b** The plots on the *upper right* show the time course of the moments modeled by the three dipoles. **c** The *lower left plot* shows the fit of the dipole solution (*dotted line*) to the scalp-surface potential (*unbroken line*) at selected electrodes. The residual variance over the time interval of 10–25 ms in this subject was 1.96%. **d** The *lower right plot* shows three orthogonal views of the dipoles that modeled the P20-N20 potential in all ten subjects

Establishment of postcentral reference from electrical stimulation of the median nerve

For the purposes of discussion, the somatosensory-evoked potentials (SEPs) generated by angular displacements of the wrist will be termed SEP_{WDs} (wrist-displacement SEPs) in order to differentiate them from the potentials evoked by electrical stimulation of the median nerve at the wrist, which will be referred to as SEP_{MNs} (median-nerve SEPs). Electrical stimulation of the median nerve at the wrist evoked SEPs that were the same in timing and topography as previous studies using a similar electrode montage and a non-cephalic or average reference (Desmedt and Cheron 1981; Buchner et al. 1995) (Fig. 2). The components of the SEP_{MNs} that were reliably present in all subjects were: P14 (1.3±1.2 μV peak at 13.5±0.9 ms), P20 (1.9±0.8 μV peak at 19.2±1.8 ms), N20 (–2.1±1.5 μV peak at 19.0±0.5 ms), P22 (1.5±0.8 μV peak at 22.4±1.6 ms), N30 (–4.1±1.7 μV peak at 30.7±3.1 ms), and P30 (4.1±1.8 μV peak at 30.4±3.6 ms).

The source generators of the early components of the SEP_{MNs} were modelled using the strategy previously described by Buchner et al. (1995). A three dipole model was sufficient to explain over 96% of the scalp-surface potential (mean RV of 4.3±3.3%) over the time interval of 14–22 ms (Fig. 3). The far-field P14-N14 potential was modelled by a source deep within the cerebrum with a mean location of x=0.9±6.1, y=–14.9±8.7, z=–29.0±13.7 and orientation of θ=–26±10°, ϕ=–83±5°. The second dipole localised to the region of the contralateral sensorimotor cortex (mean location of x=–31.8±3.6, y=–2.7±2.4, z=48.5±6.1 mm) and showed a predominantly tangential orientation (θ=68±19°, ϕ=66±13°) and a time course similar to the P20-N20 component. Accordingly, we termed this generator the P20-N20, or area 3b, dipole and used it as the local spatial reference to determine the relative location and orientation of the SEP_{WD} dipoles. The third dipole also localised to the region of the contralateral sensorimotor cortex (mean location: x=–29.3±10.1, y=3.4±7.8, z=58.1±6.3; mean orientation: θ=–83±30°, ϕ=42±25°) and explained potentials generated after 20 ms.

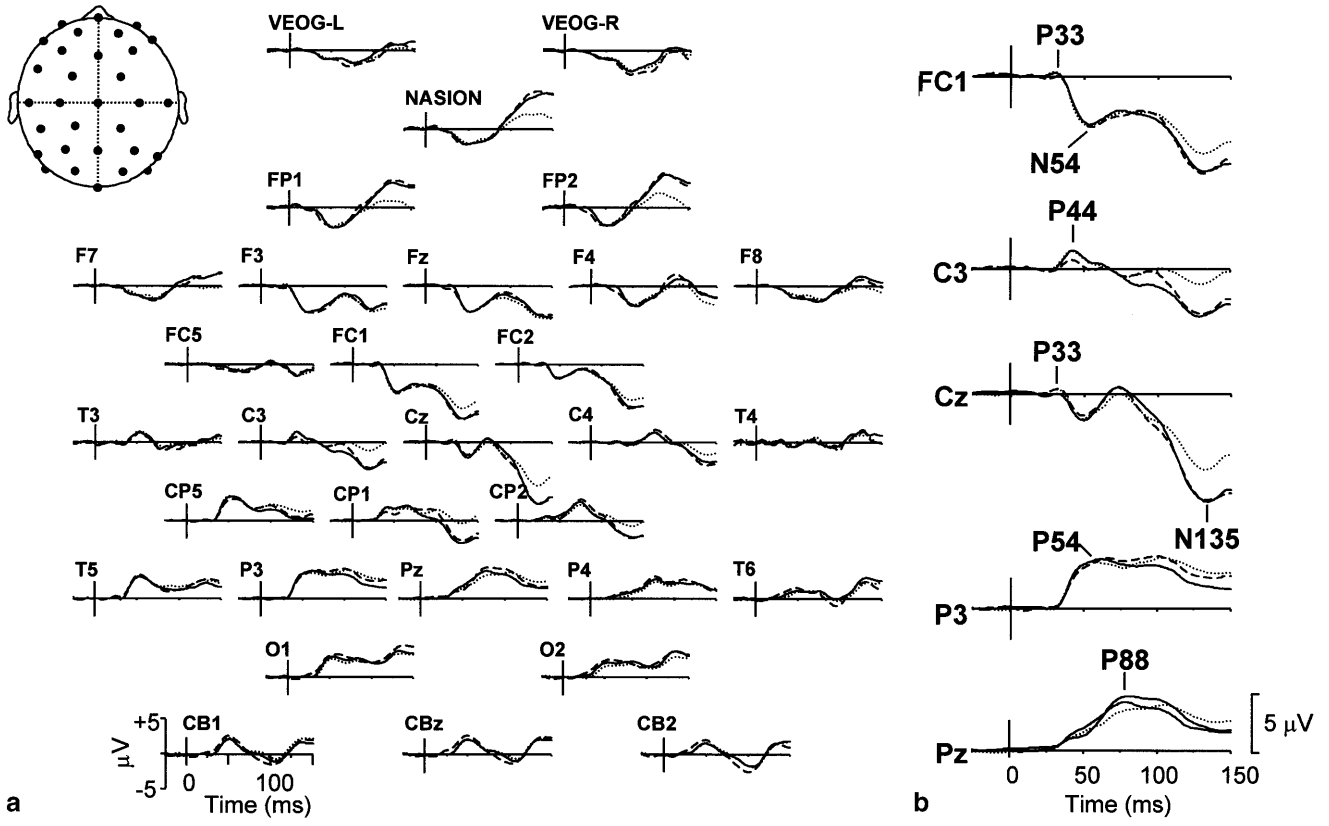

Fig. 4 a Grand average (*n*=10) scalp-surface topography of the somatosensory-evoked potentials (SEPs) elicited by imposed wrist extension displacements over the time interval of –25 to 150 ms after the onset of the step-load. The cerebral potentials at 31 electrodes encompassing the surface of the scalp are shown relative to an average reference derived from all electrodes. A schematic cartoon of the placement of the electrodes on the surface of the head is shown at the *top left*. Note the early frontal negativity at FC1, Fz and F3 and parietal positivity at CP5, CP1 and P3, corresponding to the N54-P54 potential. **b** Enlarged graphs of the potentials recorded at Cz, C3, FC1, P3 and Pz showing the individual components discussed in the text. The plots for the RESIST (*unbroken line*), EXTEND (*dashed line*) and PASSIVE (*dotted line*) tasks (see Materials and methods for task descriptions) have been superimposed to show differences in the evoked potentials across tasks. Note that the SEPs were the same across tasks up to 75 ms after the onset of the step-load. Onset of the step-load was at time = 0 ms

Somatosensory-evoked potentials to rapid angular displacements of the wrist

The topography of the grand average SEP_{WDs} for all subjects over the collection epoch from 25 ms before to 150 ms after the onset of the step-load for all three tasks is shown in Fig. 4, along with figures showing specific components of the evoked potentials. The timing and amplitudes of the early components of the SEP_{WDs} across tasks are summarised in detail in Table 1 of the Supplementary Materials section posted on the Springer-Verlag server (http://dx.doi.org/10.1007/s002219900317).

The potentials evoked by imposed joint displacements differed markedly from those evoked by electrical stimulation of the median nerve at the wrist (compare Figs. 2 and 4). The SEP_{WDs} did not show an early N14-P14 far field or P20-N20 cortical components characteristic of the SEP_{MNs}. The early components of the SEP_{WDs} were characterised by a small amplitude positivity at Cz or FC1 (termed the P33 component) with an average onset of 27 ms and a peak amplitude at Cz of 0.8 μV at 33 ms, a central positivity at CP1 (or C3) (termed the P44 component) with a mean onset latency of 32 ms and peak amplitude of 2.7 μV at 44 ms, frontal negativity at the FC1 electrode (or Fz or F3) (termed the N54 component) with an onset near 33 ms, average peak amplitude of –4.8 μV and average latency to peak of 54 ms, and a parietal positivity at P3 (or CP5) (termed the P54 component) with the same average and peak times as the N54 component and average peak amplitude of 4.7 μV. Later components consisted of a parietal positivity, which was maximal at Pz electrode with an average peak latency of 88 ms (P88 component) and an average amplitude of 4.6 μV, and a late, large amplitude (average peak amplitude for the RESIST task of –9.7 μV) and diffusely distributed negativity, which peaked at the vertex (Cz) at an average of 135 ms (N135 component).

Comparison of the SEP_{WDs} across tasks (Fig. 4) demonstrated that the timing and magnitude of the early components of the SEP_{WDs} did not differ between active and passive tasks over the time interval of 0–75 ms after the onset of the step-load. Therefore, unlike the M2 response, the early components of the SEP_{WDs} were not modulated across tasks. The N135 component was the only variable measured in association with the SEP_{WDs} that showed a significant change across tasks. The

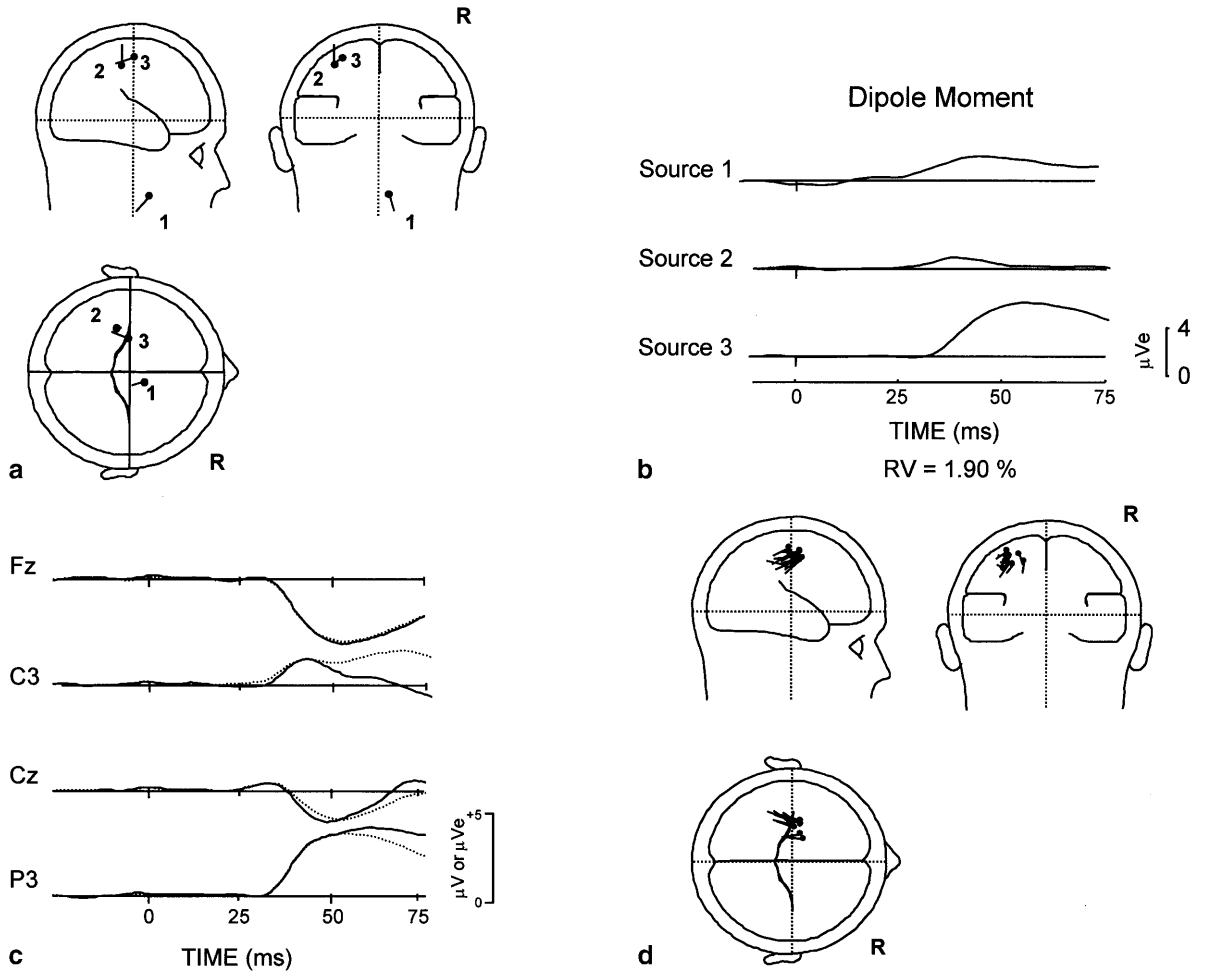

Fig. 5a–d The location and moments generated by the three dipoles (*1–3*) that modeled the early components of the wrist displacement somatosensory-evoked potentials (SEP_{WDs}) for the RESIST task (see Materials and methods for task description). **a** The head models on the *upper left* show three orthogonal views of the location and orientation of the three dipoles that modeled the scalp-surface potentials. **b** The plots on the *upper right* show the time course of the moments modeled by the three dipoles. **c** The *lower left plot* shows the fit of the dipole solution (*dotted line*) to the scalp-surface potential (*unbroken line*) at selected electrodes. **d** The *lower right plot* shows three orthogonal views of the dipoles that modeled the N54-P54 potential in all ten subjects

PASSIVE task was associated with a 25±26% and 23±25% decrease, respectively, in the amplitude of the N135 potential relative for both the RESIST (P=0.008) and EXTEND (P=0.007) tasks.

Dipole source analysis of SEP_{WDs}

Since the early evoked potentials were virtually identical in timing and magnitude at all electrodes for all three tasks, the dipole solutions were essentially the same across tasks. A three-dipole solution was required to sufficiently model the SEP_{WDs} over the time interval from the onset of the P33 to the peak of the N54-P54 component (Fig. 5a). The dipole fitting procedure is explained in detail in the Supplementary Materials section posted on the Springer-Verlag server (http://dx.doi.org/10.1007/s002219900317).

Dipole source analysis of the grand average potentials over the time interval of 28–54 ms yielded solutions with RV's of 1.9%, 1.2% and 1.8% for the RESIST, EXTEND and PASSIVE tasks, respectively (Fig. 5c). This means that over 98% of the scalp surface EEG over the 28- to 54-ms time interval was explained by the three-dipole model. The corresponding average RV's for within-subject solutions were: RESIST =4.7±2.0% (range: 2.4–9%); EXTEND =4.1±2.4% (range: 2.0–9.2%); and PASSIVE =3.8±1.1% (range: 2.4–6.2%). Beyond the fitting interval of 54 ms, the model did not adequately explain the late components of the SEP_{WDs} (RV >5%). Efforts to obtain a dipole solution beyond the 54-ms range across subjects that fulfilled the criteria outlined in the methods were unsuccessful.

The three dipoles that modelled the scalp-surface potentials over the fitting interval of 28–54 ms were a dipole deep within the cerebrum (source 1), a radially oriented dipole in the region of the contralateral postcentral cortex (source 2) and a tangential dipole near the region of the contralateral central sulcus (source 3). The location, orientation and timing of these dipoles are shown in Fig. 5 and summarised in detail in Table 2 of the Supple-

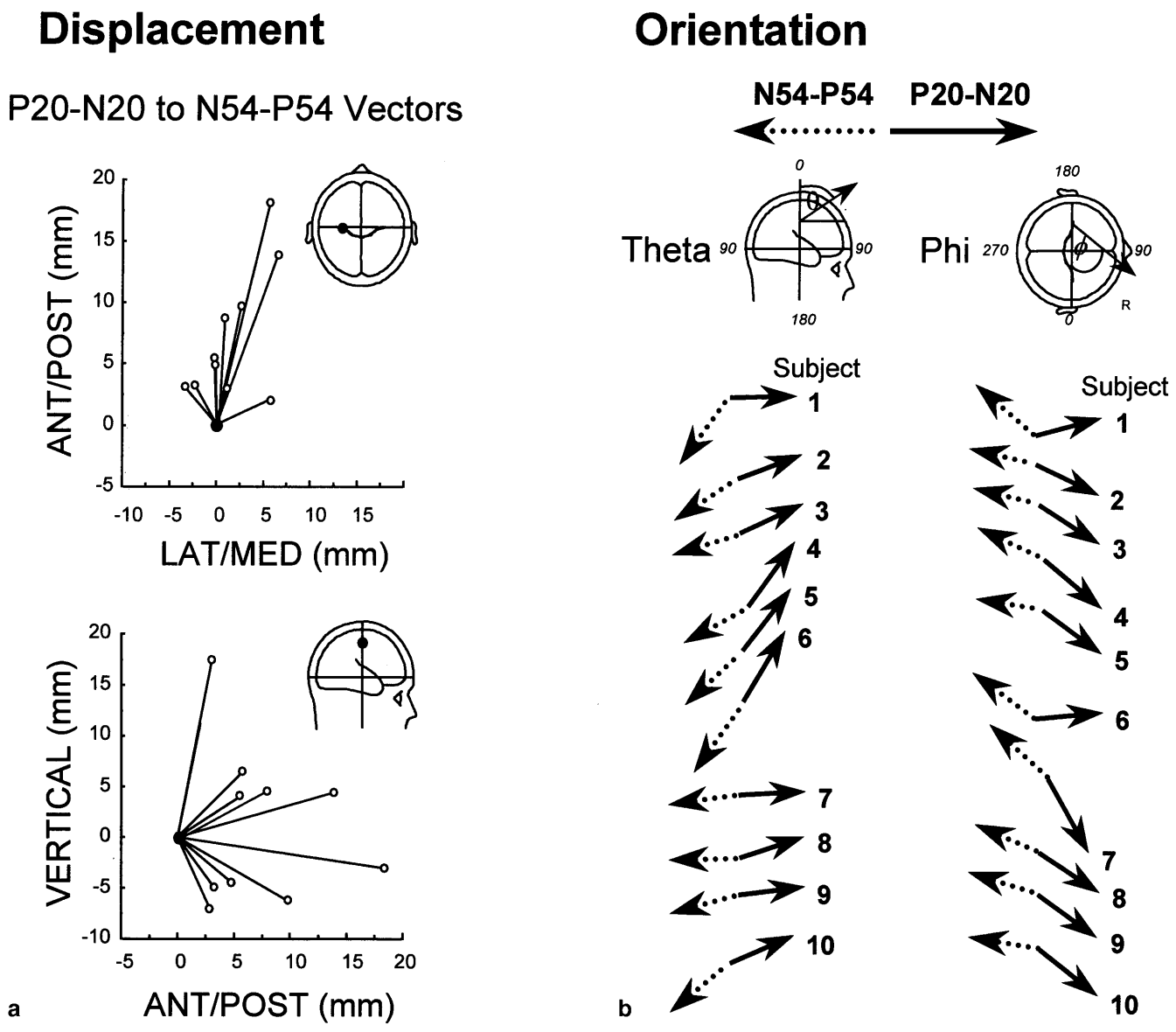

Fig. 6 **a** Plots on the *left* show vectors drawn from the location of the P20-N20 median nerve somatosensory-evoked-potential (SEP_{MN}) dipole (origin at x, y, z = 0, 0, 0) to the corresponding location of the N54-P54 dipole in the same subject. Vectors for all ten subjects are shown for the RESIST task (see Materials and methods for task description). The N54-P54 dipole was consistently located anterior to the P20-N20 dipole, whereas the medial/lateral and dorsal/ventral location was variable across subjects. On average, the N54-P54 dipole was located anterior, medial and dorsal to the P20-N20 dipole. The mean resultant vector across subjects for the RESIST task was 11.6±4.8 mm. **b** Within-subject comparisons of the orientation of the N54-P54 (*dotted arrow*) and P20-N20 (*unbroken arrow*) dipoles for the RESIST task. Unit vector pairs on the *left* show orientations of the dipoles in the sagittal plane (*theta*) for each of the ten subjects. Vector pairs on the *right* show orientations in the transverse plane (*phi*). Note that the N54-P54 and P20-N20 vectors were not oppositely oriented for theta or phi. Vectors were given a common origin for comparative purposes only

mentary Materials section posted on the Springer-Verlag server (http://dx.doi.org/10.1007/s002219900317).

Source 1 consistently localised deep within the cerebrum. Due to the high variability in the location and orientation of this dipole across subjects, a specific subcortical region associated with the generation of this potential could not be discerned. The P44 component of the SEP_{WDs} was best explained by a predominantly radially oriented dipole located in the region of the contralateral postcentral cortex (source 2). This dipole was observed in only five of ten subjects, but was present in the grand average dipole solutions for each task. In some subjects (n=3), the radial dipole was located deep and lateral to the tangential P20-N20 dipole, whereas in other subjects the dipole localised to the cortical surface and posterior to the tangential sensorimotor cortical dipole (n=2).

Dipole solutions consistently (ten of ten subjects) included a dipole that localised to the region of the contralateral sensorimotor cortex and adopted a predominantly tangential orientation relative to the scalp surface (source

3) (Fig. 5d). The dipole moment had an average onset near 35 ms, increased in magnitude to an average peak amplitude of 4.7 μVe near 54 ms and had a temporal profile similar to the N54 and P54 scalp-surface potentials. For this reason, we termed this source the N54-P54 dipole. The average location (x=–31.7, y=3.1, z=50.6 mm) and orientation (θ=102.7°, ϕ=244.2°) of this dipole appeared to be consistent with activity originating from within the anterior or posterior banks of the central sulcus, but this analysis alone was not sufficient to determine the localisation of the N54-P54 dipole.

Localisation of the sensorimotor dipole generator

Both the P20-N20 and N54-P54 dipoles consistently localised to the lateral convexity of the central sulcus at approximately the same depth within the cerebrum, but with opposite dipole polarities (Figs. 3d and 5d). Since the location of P20-N20 is known to be generated by synaptic input to neurones in area 3b on the posterior bank of the central sulcus, we compared the relative location and orientation of the P20-N20 and N54-P54 dipoles for each subject. Vectors were calculated from an origin at the location of the P20-N20 dipole to the corresponding N54-P54 dipole location for each subject. Figure 6a shows the vectors determined for each subject for the RESIST task. The relative vertical and medial/lateral position of the N54-P54 dipole dipoles was variable across subjects with mean locations 1.7±3.6 mm medial and 1.3±8.6 mm dorsal to the P20-N20 origin for the RESIST task and 0.8±6.1 mm medial and 2.1±4 mm dorsal for the PASSIVE task. The vertical and medial/lateral positions of the N54-P54 and P20-N20 dipoles were not significantly different (P>0.6). In contrast, the N54-P54 dipoles were located anterior to the P20-N20 dipole for all subjects and for all tasks. The anterior/posterior location of the P20-N20 and N54-P54 dipoles were significantly different (P=0.02 RESIST task, P=0.02 EXTEND task, P=0.004 PASSIVE task), with average distances between them of 7.0±5.7, 8.1±4.5 and 7.5±3.8 mm for the RESIST, EXTEND and PASSIVE tasks, respectively. The mean resultant distances between the P20-N20 and N54-P54 dipoles were 11.6±4.8 mm, 11.1±5.6 mm and 11.7±5.2 mm for the RESIST, EXTEND and PASSIVE tasks, respectively. This displacement places the N54-P54 dipole within the anterior bank of the central sulcus (Talairach and Tournoux 1988; Zilles et al. 1995; White et al. 1997).

We also conducted within-subject comparisons of the orientations of the P20-N20 and N54-P54 dipole vectors (Fig. 6b). The average angles of the P20-N20 and N54-P54 dipole vectors relative to the vertical axis (θ) were 68 and 103° for the P20-N20 and N54-P54 dipoles, respectively, and relative to the medial-lateral axis (ϕ) were 66 and 244°, respectively. Opposite dipole orientations might represent a reversal in the polarity of extracellular currents generated in area 3b (cortical surface-negative, deep-positive). Accordingly, the N54-P54 vector would be precisely opposite in orientation relative to the P20-N20 dipole in the same subject. Figure 6b shows that the two vectors were not oppositely oriented in any of the ten subjects. Differences in orientation would be expected for separate generators within adjacent portions of cortical areas 3b and 4 due to asymmetries in cortical enfolding. In summary, the N54-P54 dipole differed in both location and orientation to the P20-N20 dipole and corresponded most closely to a generator within area 4 on the anterior bank of the central sulcus and not within cortical areas 3b or 3a.

Discussion

The principal finding of these experiments was the demonstration that an early component of the potentials evoked by imposed displacements of the human wrist is generated by synaptic activity within the primary motor cortex. The following discussion will consider the validity of our conclusion that the location, orientation and timing of the postsynaptic potentials modelled by the N54-P54 dipole was appropriate to represent synaptic input onto corticospinal neurones in the precentral gyrus, whose descending action potential volleys contribute to the generation of the M2 response. In addition, we found that the early components of the wrist displacement potentials did not demonstrate task-dependent modulation despite a marked variation in the magnitude of the M2 response across tasks. The absence of changes in the timing or magnitude of the short-latency SEP_{WDs} across tasks suggests that synaptic inputs to the sensorimotor cortex saturated at the velocities imposed in the present experiments and that modulation of the M2 occurs downstream from inputs to the primary motor cortex.

Somatosensory-evoked potentials to imposed displacement of the wrist

Experiments in monkeys have established that afferent volleys evoked by imposed displacements of the distal upper limb ascend to the cortex via dorsal column, medial lemniscal, thalamocortical pathways, resulting in the discharge of motor cortical neurones contralateral to the imposed displacement (Wiesendanger and Miles 1982). Dipole source analysis of the SEP_{WDs} yielded source generators that appeared to be consistent with these pathways.

The earliest components of the SEP_{WDs} appeared to represent a deep subcortical generator and a radial generator in the region of the contralateral postcentral cortex. The deep subcortical dipole might reflect inputs to the dorsal column or thalamic relay neurones, but, due to the high variability in the location and orientation of this dipole across subjects, a specific region could not be identified. Increasing the extent and density of electrodes surrounding the brain stem may improve the localisation of this source.

The P44 component of the SEP_{WDs} was best explained by a radially oriented dipole in the region of the contralateral postcentral cortex. The location of this dipole relative to the P20-N20 dipole varied across subjects, ranging from a position directly ventral to the P20-N20 dipole (three subjects) to posterior and near the surface of the postcentral cortex (two subjects). The P44 component appeared to be analogous to the P34 and P1 components previously described by Desmedt and Ozaki (1991) and Mima et al. (1996), respectively. They proposed that this potential may reflect the arrival of mechanoreceptive afferent volleys to areas 3a, 1 and 2 of the primary somatosensory cortex. The postcentral location and radial orientation of this dipole appears to support this interpretation.

The most conspicuous components evoked by imposed displacements of the wrist were the N54 and P54 potentials. The time course of these components were most closely modelled by a tangentially oriented dipole that localised to coordinates within the head model (average location =–32, 3, 51 mm) compatible with a generator deep within the banks of the central sulcus (Talairach and Tournoux 1988).

The average resultant displacement between the P20-N20 and the N54-P54 dipoles was 11.5 mm, which placed the N54-P54 within the region of the anterior bank of the central sulcus. We estimated the distance between the deep cortical layers of the forearm and hand regions of cortical area 3b and the adjacent caudal area 4 on the anterior bank of the central sulcus, based on sagittal brain sections from human cadavers, measurements from a set of high-resolution MRI T2-weighted images (n=3) and reports of sensorimotor cortical thickness in humans (Zilles et al. 1995). Distance estimates from layer III of area 3b to the adjacent layer V of area 4 averaged 11.9 mm and corresponded closely to the resultant distance of approximately 11.5 mm calculated in this study.

The orientation of the N54-P54 dipole was also compatible with synaptic input to neurones within the banks of the central sulcus. Comparisons between the N54-P54 and P20-N20 dipoles showed that they were not oppositely oriented. An opposite orientation of the N54-P54 would have suggested that the source generator may reflect a reversal of the currents associated with synaptic input to neurons in area 3b (the second phase of the P20-N20 input). The differences in orientation of the N54-P54 and P20-N20 dipoles appeared to be compatible with the within-subject differences in enfolding of the posterior and anterior banks of the central sulcus near the region of hand representation (White et al. 1997). Alternatively, differences in orientation could be accounted for by the effects of overlapping activity from other sources. Therefore, differences in orientation may be a necessary, but not sufficient, argument for two separate generators.

The N54-P54 component identified in the present study appears to be analogous to the N30 component of the median nerve SEPs. Two studies have presented evidence that the N30 component is likely generated by synaptic input to neurones within the anterior bank of the central sulcus (Peterson et al. 1995; Waberski et al. 1999). Similar to our findings for the N54-P54 dipole, the N30 dipole has been shown to have a predominantly tangential orientation and to be located anterior, medial and dorsal to the P20-N20 dipole (Kawamura et al. 1996; Waberski et al. 1999). The relative localisation of both the N54-P54 and N30 dipoles, therefore, appear to be consistent with the oblique anterior-to-posterior, medial-to-lateral, dorsal-to-caudal course of the central sulcus.

Our findings differ from the interpretation of the frontal-negative partial-positive potentials described in previous studies examining potentials evoked by displacements of the interphalangeal joints (Desmedt and Ozaki 1991; Mima et al. 1996). These studies proposed that the frontal and parietal components were generated by separate sources within the postcentral (areas 3a or 2) and frontal cortex, based on differences in the timing of the components and differences in modulation with changes in the velocity of the displacement. The SEP_{WDs} recorded in the present study did not show any consistent within-subject differences in the onsets or peak latencies of the N54 and P54 components. Discrepancies in the parietal and frontal potentials reported previously, compared with those in the present study, might be explained by differences in the magnitude and timing of the afferent volley evoked by the imposed joint displacement. Our data show that the time course of the postcentral and N54-P54 dipole moments overlapped extensively. This results in a summation of the positive potentials over the contralateral parietal cortex. An increase in the magnitude of the postcentral potential, due to increased spatial or temporal summation of postsynaptic potentials to neurones in the somatosensory cortex (areas 3a, 1 or 2), could result in an earlier peak in the parietal waveform. Given the high density of muscle spindles within the muscles controlling the interphalangeal joints of the human hand, the early peak in the parietal waveform reported by Desmedt and Osaki (1991) might be explained by a larger, more coherent volley of fast-conducting muscle-afferent input to the postcentral cortex that superimposes on the potentials generated by input to neurones in the primary motor cortex.

Bötzel et al. (1997) have previously used dipole source analysis to examine the source generators of the potentials evoked by manually imposed distal joint displacements. Similar to our findings, they showed that a single, tangentially oriented dipole in the region of the contralateral sensorimotor cortex provided a good model of the frontal-negative parietal-positive (N54-P54) complex. The authors concluded, based on the location and orientation of the sensorimotor dipole, that the dominant source generator was likely located within the primary somatosensory cortex, principally area 3a, but did not rule out a possible primary motor cortex generator within the anterior wall of the central sulcus. However, the tangential orientation of the passive movement dipole did not appear to be compatible with a generator within area

3a, considering that postsynaptic potentials arising from deep within the fundus of the central sulcus would be expected to have a predominantly radial orientation. Furthermore, the authors were unable to account for the finding that the passive-movement dipole was located, on average, 8 mm posterior and 10 mm medial to the P20-N20 generator. This might be explained by the modelling strategy adopted by Bötzel et al. (1997), which used only a single dipole to account for the potentials evoked over the long time interval of 50–250 ms after the onset of movement. Therefore, the location of the passive movement dipole may have been affected by additional, temporally overlapping source generators.

The spatial and temporal characteristics of the potentials evoked by imposed joint displacement differ markedly from the potentials evoked by electrical stimulation of the median nerve at the wrist (see Figs. 2 and 4 and Desmedt and Osaki 1991; Mima et al. 1996, 1997). These differences are thought to reflect a marked increase in the activation of fast-conducting deep mechanoreceptive afferents (principally group 1a) with joint displacements relative to the fast-conducting cutaneous afferents activated by surface electrical stimulation. In fact, cerebral potentials consistent in location and timing to those reported in the present study have been reported in response to intramuscular microstimulation of the motor points of distal upper-limb muscles (Gandevia et al. 1984). Similarly, the long-latency EMG activity evoked in the wrist muscles of humans have been shown to be mediated by deep sensory afferents and not cutaneous inputs (Bawa and McKenzie 1981). Taken together, these findings suggest that the early components of the potentials evoked by imposed displacements of distal upper-limb joints are principally mediated by ascending volleys from fast-conducting mechanoreceptive afferents.

Timing of the motor cortical potential

We examined the timing of the N54-P54 dipole moment to estimate if this activity was appropriate for synaptic activity onto corticospinal neurones that participate in the generation of the M2 response. The minimum delay from the onset of the peripheral afferent volley to arrival at the contralateral somatosensory cortex is 17–20 ms (Desmedt and Cheron 1981, 1982). Similarly, the minimum conduction delay from the onset of the corticospinal volley to the onset of EMG activity in FCR is approximately 17 ms (Lemon 1993). The average latency of the M2 responses in the present study was 53 ms (accounting for a torque motor rise time of approximately 3–4 ms and an additional 5–6 ms resulting from coupling and inertial delays) (Bedingham and Tatton 1984). Therefore, the latest onset time for the initiation of the corticospinal volley that generates M2 would be 36 ms. The N54-P54 dipole moment had an average onset latency of 27 ms (corrected for torque motor delays), 20 ms rise-time and latency to peak of 48 ms. The onset of the N54-P54 dipole moment occurred approximately 8 ms after the arrival of the afferent volley to the somatosensory cortex and 9 ms before the latest possible onset time of the descending corticospinal volley. The delays between sensory afferent input and motor efferent output can be accounted for by cortico-cortical axonal conduction and synaptic delays between areas 3a and 2, and summation and rise times of the post-synaptic-membrane potentials at the linking and target neurones (Ghosh and Porter 1988). Allowing for errors in estimates of the onset and synaptic delays to the motor cortex, the timing of the N54-P54 dipole moment could reflect synaptic activity onto motor-cortical neurones whose descending volleys result in excitation of spinal motoneurones that contribute to the M2. Alternatively, the 5-ms difference between the timing of the afferent-efferent loop times might result from slower-conducting corticospinal neurones or a polysynaptic pathway linking the descending corticospinal volley and excitatory inputs to the α-motoneurone.

An alternative approach to examining the relationship between the timing of the motor cortical potential and the M2 response is to back-average the cerebral potentials from the onset of the M2. The onset of the M2 could be reliably distinguished from the earlier EMG activity in a sufficient number of trials for back-averaging (182 trials from all three tasks) in only one subject. This procedure revealed a distinct potential that preceded the onset of the M2 by 35 ms and had a scalp-surface topography similar to the N54-P54 potential (peak frontal negativity at FC1, peak parietal positivity at P3 and reversal over the contralateral sensorimotor cortex). The peak of this potential (4 ms after M2 onset) was modelled by a dipole that localised to the same region (x, y, z = –30.2, 0.1, 55.2 mm) and had a similar orientation (θ=96.9°, ϕ=258.6°) to the N54-P54 dipole. This dipole alone accounted for 94.1% of the variance between the scalp surface EEG and the dipole model. These results further support the premise that activity within the motor cortex is time-locked to the onset of the M2.

Task-dependent modulation of M2, but not SEP_{WDs}

One of the unexpected results of these experiments was the absence of modulation in the timing and magnitude of the early SEP_{WDS}, despite marked variation in the magnitude of the M2 responses across tasks. The absence of modulation of the SEP_{WDs} across tasks may reflect a saturation of the evoked potentials at the velocities imposed in the present experiments. Previous studies have shown that the relationship between the size of electrically induced afferent volleys and the magnitude of the early evoked cerebral potential is highly non-linear (Gandevia et al. 1982; Gandevia and Burke 1984). Cerebral potentials evoked by electrical stimulation of cutaneous or muscle afferents reach a plateau when the afferent volley has reached only 50% of its maximum size. Abbruzzese et al. (1985) reported a velocity-dependent modulation of the early cerebral potentials evoked by imposed wrist displacements over a range of

100–300°/s. The peak velocities used in the present study were over twice the rate reported by Abbruzzese et al. Without systematic testing of the evoked potentials over a range of velocities, it could not be determined if the afferent volley evoked by the joint displacements in the present study was sufficient to saturate the SEP_{WDs}.

Nonetheless, the fact that the early components of the SEP_{WDs} were not modulated across tasks, despite a marked gradation of the M2 response, provides further indirect evidence that the M2 evoked in the wrist flexors of humans is mediated by more than one pathway. Experiments examining the effects of displacement duration have shown that the FCR M2 is absent for displacements of less than approximately 44 ms (Lee and Tatton 1982). The time difference between the critical duration of the imposed displacement and the onset of the M2 suggested that the response was dependent upon inputs from two or more convergent pathways: a long-latency transcortical and a slow-conducting or polysynaptic segmental pathway. Accordingly, modulation of the M2 response could occur downstream from inputs to the motor cortex by acting on interneurons interposed between descending corticospinal or segmental inputs to the α-motoneuron. Descending influences initiated during the premovement period could be mediated by neurones in the primary motor cortex, premotor cortex (e.g., Tanji and Evarts 1976) or supplementary motor area (Tanji and Kurata 1985; Romo and Schultz 1992).

Acknowledgements The authors thank Cindy Major, Phyllis Clarke and Chanh Diep for technical assistance with the project. CDM was supported by a fellowship from the Ontario Ministry of Health.

References

Abbruzzese G, Berardelli A, Rothwell JC, Day BL, Marsden CD (1985) Cerebral potentials and electromyographic responses evoked by stretch of wrist muscles in man. Exp Brain Res 58:544–551

Ackermann H, Diener HC, Dichgans J (1986) Mechanically evoked cerebral potentials and long-latency muscle responses in the evaluation of afferent and efferent long-loop pathways in humans. Neurosci Lett 66:233–238

Allison T, McCarthy G, Wood CC, Jones SJ (1991) Potentials evoked in human and monkey cerebral cortex by stimulation of the median nerve. Brain 114:2465–2503

Bawa P, McKenzie DC (1981) Contribution of joint and cutaneous afferents to long-latency reflexes in man. Brain Res 211:185–189

Bedingham W, Tatton WG (1984) Dependence of EMG responses evoked by imposed wrist displacement on pre-existing activity in the stretched muscles. Can J Neurol Sci 11:272–280

Bötzel K, Ecker C, Schulze S (1997) Topography and dipole analysis of reafferent electrical brain activity following the Bereitschaftspotential. Exp Brain Res 114:352–361

Buchner H, Adams L, Muller A, Ludwig I, Knepper A, Thron A, Niemann K, Scherg M (1995) Somatotopy of human hand somatosensory cortex revealed by dipole source analysis of early somatosensory evoked potentials and 3D-NMR tomography. Electroencephalogr Clin Neurophysiol 96:121–134

Cheney PD, Fetz EE (1984) Corticomotoneuronal cells contribute to long-latency stretch reflexes in the rhesus monkey. J Physiol 349:249–272

Conrad B, Dressler D, Benecke R (1984) Changes of somatosensory evoked potentials in man as correlates of transcortical reflex modulation? Neurosci Lett 46:97–102

Crammond DJ, MacKay WM, Murphy JT (1985) Evoked potential from passive movements. I. Quantitative spatial and temporal analysis. Electroencephalogr Clin Neurophysiol 61:396–410

Day BL, Riescher H, Struppler A, Rothwell JC, Marsden CD (1991) Changes in the response to magnetic and electrical stimulation of the motor cortex following muscle stretch in man. J Physiol 433:41–57

Desmedt JE, Cheron G (1981) Non-cephalic reference recording of early somatosensory potentials to finger stimulation in adult or aging normal man: differentiation of widespread N18 and contralateral N20 from the prerolandic P22 and N30 components. Electroencephalogr Clin Neurophysiol 52:553–570

Desmedt JE, Cheron G (1982) Somatosensory evoked potentials in man: subcortical and cortical components and their neural basis. Ann N Y Acad Sci 388:388–411

Desmedt JE, Ozaki I (1991) SEPs to finger joint input lack the N20-P20 response that is evoked by tactile inputs: contrast between cortical generators in area 3b and 2 in humans. Electroencephalogr Clin Neurophysiol 80:513–521

Fellows SJ, Töpper R, Schwarz M, Thilmann AF, Noth J (1996) Stretch reflexes of the proximal arm in a patient with mirror movements: absence of bilateral long-latency components. Electroencephalogr Clin Neurophysiol 101:79–83

Gandevia SC, Burke D (1984) Saturation in human somatosensory pathways. Exp Brain Res 54:582–585

Gandevia SC, Burke D, McKeon B (1982) The relationship between the size of a muscle afferent volley and the cerebral potential in produces. J Neurol Neurosurg Psychiatry 45:705–710

Gandevia SC, Burke D, McKeon B (1984) The projection of muscle afferents from the hand to cerebral cortex in man. Brain 107:1–13

Ghosh S, Porter R (1988) Corticocortical synaptic influences on morphologically identified pyramidal neurons in the motor cortex of the monkey. J Physiol 400:617–629

Goodin DS, Aminoff MJ (1992) The basis and functional role of the late EMG activity in human forearm muscles following wrist displacement. Brain Res 589:39–47

Goodin DS, Aminoff MJ, Shih PY (1990) Evidence that the long-latency responses of the human wrist extensor muscle involve a transcerebral pathway. Brain 113:1075–1091

Grimm C, Schreiber A, Kristeva-Feige R, Mergner T, Hennig J, Lücking C (1998) A comparison between electric source localisation and fMRI during somatosensory stimulation. Electroencephalogr Clin Neurophysiol 106:22–29

Hammond PH (1954) Involuntary activation in biceps following sudden application of velocity to the abducted forearm. J Physiol 127:23P–25P

Kawamura T, Nakasato N, Seki K, Kanno A, Fujita S, Fujiwara S, Yoshimoto T (1996) Neuromagnetic evidence of pre- and post-central cortical sources of somatosensory evoked responses. Electroencephalogr Clin Neurophysiol 100:44–50

Kristeva-Feige R, Grimm C, Huppertz H-J, Otte M, Schreiber A, Jäger D, Feige B, Büchert M, Hennig J, Mergner T, Lücking C (1997) Reproducibility and validity of electric source localisation with high-resolution electroencephalography. Electroencephalogr Clin Neurophysiol 103:652–660

Lee RG, Tatton WG (1975) Motor responses to sudden limb displacements in primates with specific CNS lesions and in humans patients with motor system disorders. Can J Neurol Sci 2:285–293

Lee RG, Tatton WG (1982) Long latency reflexes to imposed displacements of the human wrist: dependence on duration of movement. Exp Brain Res 45:207–216

Lemon RN (1993) Cortical control of the primate hand. Exp Physiol 78:263–301

Lenz F, Tatton W, Tasker R (1983a) Electromyographic response to displacement of different forelimb joints in the squirrel monkey. J Neurosci 3:783–794

Lenz F, Tatton W, Tasker R (1983b) The effect of cortical lesions on the electromyographic response to joint displacement in the squirrel monkey forelimb. J Neurosci 3:795–805

MacKinnon CD, Kapur S, Hussey D, Verrier MC, Houle S, Tatton WG (1996) Contributions of the mesial frontal cortex to the premovement potentials associated with intermittent hand movements in humans. Hum Brain Map 4:1–20

Marsden CD, Merton PA, Morton HB, Adam J (1977) The effect of lesions of the sensorimotor cortex and capsular on servo responses from the human long thumb flexor. Brain 100:503–526

Matthews PBC (1991) The human stretch reflex and the motor cortex. Trends Neurosci 14:87–91

Mima T, Terada K, Maekawa M, Nagamine T, Ikeda A, Shibasaki H (1996) Somatosensory evoked potentials following proprioceptive stimulation of finger in man. Exp Brain Res 111:233–245

Mima T, Ikeda A, Terada K, Yazawa S, Mikuni N, Kunieda T, Taki W, Kimura J, Shibasaki H (1997) Modality-specific organization for cutaneous and proprioceptive sense in human primary sensory cortex studied by chronic epicortical recording. Electroencephalogr Clin Neurophysiol 104:103–107

Palmer E, Ashby P (1992) Evidence that a long latency stretch reflex in humans is transcortical. J Physiol 449:429–440

Papakostopoulos D, Cooper R, Crow H (1974) Cortical potentials evoked by finger displacement in man. Nature 252:582–584

Peterson NN, Schroeder CE, Arezzo JC (1995) Neural generators of early cortical somatosensory evoked potentials in the awake monkey. Electroencephalogr Clin Neurophysiol 96: 248–260

Romo R, Schultz W (1992) The role of primate basal ganglia and frontal cortex in the internal generation of movements. III. Neuronal activity in the supplementary motor area. Exp Brain Res 91:396–407

Scherg M (1990) Fundamentals of dipole source potential analysis. In: Grandori F, Hoke M, Romani GL (eds) Auditory evoked magnetic fields and electric potentials. Advances in audiology, vol 6S. Karger, Basel, pp 40–69

Siegel S (1956) Non-parametric statistics for the behavioural sciences. McGraw-Hill, New York

Talairach J, Tournoux P (1988) Co-planar stereotaxic atlas of the human brain. Translated by Rayport. M. Thieme Medical, New York

Tanji J, Evarts EV (1976) Anticipatory activity of motor cortex neurons in relation to direction of an intended movement. J Neurophysiol 39:1062–1068

Tanji J, Kurata K (1985) Contrasting neuronal activity in supplementary and precentral motor cortex of monkeys. I. Responses to instructions determining motor responses to forthcoming signals of different modalities. J Neurophsyiol 53:129–141

Tarkka IM, Hallett M (1991) Topography of scalp-recorded motor potentials in human finger movements. J Clin Neurophysiol 8:331–341

Tatton WG, Lee RG (1975) Evidence for abnormal long-loop reflexes in rigid Parkinsonian patients. Brain Res 100:671–676

Tatton WG, Forner SD, Gerstein GL, Chambers WW, Liu CN (1975) The effect of postcentral cortical lesions on motor responses to sudden upper limb displacements in monkeys. Brain Res 96:108–111

Tatton WG, North AGE, Bruce IC, Bedingham W (1983) Electromyographic and motor cortical responses to imposed displacements of the cat elbow: disparities and homologies with those of the primate wrist. J Neurosci 3:1807–1817

Thilmann AF, Schwarz M, Töpper R, Fellows SJ, Noth J (1991) Different mechanisms underlie the long-latency stretch reflex response of active human muscle at different joints. J Physiol 444:631–643

Verrier MC, Tatton WG, Blair RDG (1984) Characteristics of EMG responses to imposed limb displacements in patients with vascular hemiplegia. Can J Neurol Sci 11:288–296

Waberski TD, Buchner H, Perkuhn M, Gobbelé R, Wagner M, Kücker W, Silny J (1999) N30 and the effect of explorative finger movements: a model of the contribution of the motor cortex to early somatosensory potentials. Clin Neurophysiol 110:1589–1600

Wiesendanger M, Miles TS (1982) Ascending pathway of low-threshold muscle afferents to the cerebral cortex and its possible role in motor control. Physiol Rev 62:1234–1270

White LE, Andrews TJ, Hulette C, Richards A, Groelle M, Paydardar J, Purves D (1997) Structure of the human sensorimotor system: morphology and cytoarchitecture of the central sulcus. Cereb Cortex 7:18–30

Zilles K, Schlaug G, Matelli M, Luppino G, Schleicher A, Qü M, Dabringhaus A, Seitz R, Roland PE (1995) Mapping of human and macaque sensorimotor areas by integrating architectonic, transmitter receptor, MRI and PET data. J Anat 187:515–537